A New Fault-Tolerant Flux-Reversal Doubly-Salient Magnetless Motor Drive with Four-Phase Topology

Christopher H. T. Lee[1,2], *Student Member, IEEE*, K. T. Chau[1,2], *Fellow, IEEE*, and Chunhua Liu[1,2], *Senior Member, IEEE*,
1. Shenzhen Institute of Research and Innovation, The University of Hong Kong, Shenzhen, China
2. Department of Electrical and Electronic Engineering, The University of Hong Kong, Hong Kong, China
E-mail: ktchau@eee.hku.hk

***Abstract*--The proposed fault-tolerant flux-reversal doubly-salient (FT-FRDS) magnetless motor drive consists of armature winding for driving and DC-field winding for field excitation. The purpose of this paper is to investigate two remedial strategies for fault-tolerant operations of the proposed motor drive under short-circuit faults. First, short-circuit phase can be disabled and the short-circuit fault can then be regarded as the open-circuit fault. By reconstructing the healthy armature phases, the reduced torque can be remedied and this is known as the fault-tolerant brushless AC (FT-BLAC) operations. Second, short-circuit fault can also be remedied based on the DC-field regulation alone, and this is known as the fault-tolerant DC-field (FT-DC) operation. These two remedial operations are compared and verified by the finite-element-method (FEM).**

***Index Terms*--Fault-tolerant, flux-reversal, doubly-salient, magnetless, multi-phase, electric machine, renewable energy, cost-effectiveness.**

I. Introduction

ENVIRONMENTAL protection and energy efficiency have been the hot research topics in the last few decades, and hence there is the enhancing interest in the development of the electric machines [1]–[4]. Basically, the electric machines have to offer high efficiency, high power density, high controllability, wide-speed range, and maintenance-free operation [5]–[9]. The permanent-magnet (PM) machines, which achieve all these goals, have been actively developed [10]–[14]. However, the manufacturing cost of the PM materials has surged drastically due to limited and unsteady supply [15]–[18]. Hence, the advanced magnetless machines, which enjoy the higher cost-effectiveness, have started to gain more attentions recently [19]–[24]. Particularly, the magnetless flux-reversal doubly-salient (FRDS) machine, which offers attractive performances, has been suggested [25], [26]. However, the previous researches focus only on the machine standard performances, while the fault tolerance capability has not been widely discussed yet.

This work was supported in part by a grant (Project No. HKU710711E) from the Hong Kong Research Grants Council, Hong Kong Special Administrative Region, China and a grant of Basic Research Program (Project Code: CYJ20120831142942515), Science, Technology and Innovation Commission of Shenzhen Municipality, China.

To provide the more comprehensive studies of the electric machines, fault tolerance performances should also be included. Traditionally, when there is any short-circuit fault, the faulty phase can be disabled and remedied with the open-circuit fault-tolerant operation [27]–[29]. However, the conventional approach purposely boosting up the remaining healthy armature sets for torque compensations [30]–[32]. Hence, all the armature sets are required to design with the higher tolerant factors, resulting in the increased material costs. To improve the case, the controllable DC-field excitation can be instead regulated, resulting the remediation of the faulty situation without boosting the healthy armature sets [33]. This approach can optimize the design factor of the armature sets and hence improving the system performances. The DC-field regulating idea was proposed, yet the quantitative comparison between the two methods has never been suggested.

The purpose of this paper is to propose the new four-phase fault-tolerant flux-reversal doubly-salient (FT-FRDS) motor drive. To be specific, the two remedial strategies for the short-circuit faults, namely the fault-tolerant brushless AC (FT-BLAC) operation and the fault-tolerant DC-field (FT-DC) operation will be investigated. The former approach relies on the remediation of the armature sets, while the latter one is on the DC-field regulation. These two remedial operations will be discussed and compared by using the finite-element-method (FEM).

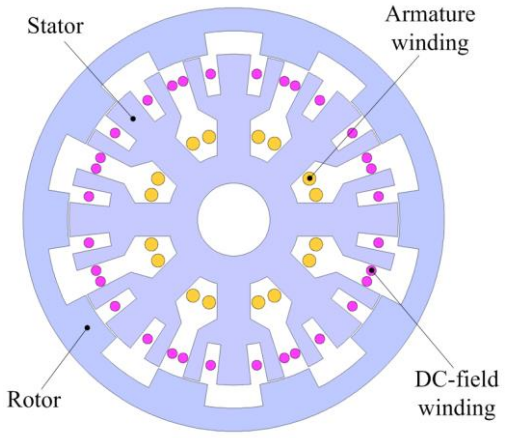

(a)

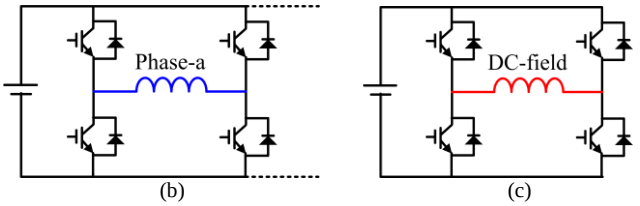

Fig. 1. Proposed FT-FRDS motor drive: (a) Machine topology. (b) Armature current controller. (c) DC-field current controller.

II. Proposed FT-FRDS Motor Drive

Fig. 1 shows the proposed FT-FRDS motor drive and the motor composes of a four-phase 8/10-pole structure. It consists of 8 salient poles in the inner stator and 10 salient poles in the outer rotor. Conventionally, the FRPM machine installs the alternating PMs on each of its stator pole, hence offering the reversing flux-linkage in accordance to its rotor positions [10]. To achieve the reversing flux-linkage characteristic, the proposed FT-FRDS machine purposely modulates its stator pole as the 3-tooth per stator pole structure, in order to accommodate the DC-field winding to provide the corresponding patterns.

The proposed motor drive adopts two types of winding, namely the armature winding and the DC-field winding. The armature current controller utilizes a four-phase full-bridge inverter to achieve independent control algorithm among phases. Meanwhile, the DC-field current controller adopts an H-bridge converter to regulate both the magnitude and direction of the DC-field excitation, hence controlling the airgap flux density.

The proposed FT-FRDS motor drive possesses several distinctions for fault-tolerant operation:

- The solid outer rotor simply consists of salient pole with no PMs or windings, hence offering high mechanical robustness and high reliability.
- The use of four-phase of the proposed motor can allow for fault-tolerant operation under losses of two phases, hence improving the reliability of the whole system.
- The concentrated armature windings can offer good magnetic independence among phase.
- The full-bridge inverter topology provides good electrical independence for the armature windings [30].
- By regulating the controllable DC-field excitation, the proposed motor drive can remedy the short-circuit fault without boosting the armature sets.

III. Remedial Operations

There are several types of short-circuit faults occur in the common motor drive and the most common one is the inter-turn winding short-circuit fault [30]. The inter-turn winding fault will be focused in this paper and it can be described by the transformer equivalent circuit as:

$$\begin{cases} u = Ri + e = Ri + N\dfrac{d\phi}{dt} \\ e_{sc} = N_{sc}\dfrac{d\phi}{dt} = R_{sc}i_{sc} \end{cases} \tag{1}$$

where Φ is the flux per phase, e and e_{sc} the induced electromotive forces (EMFs) in the phase winding and short-circuit winding, i_{sc} the current in the short-circuit winding, N and N_{sc} the numbers of turns of the phase winding and short-circuit winding, and R_{sc} the resistance of the short-circuit winding. Furthermore, they yield:

$$\frac{e_{sc}}{e} = \frac{N_{sc}}{N},\ \frac{R_{sc}}{R} = \frac{N_{sc}}{N} \tag{2}$$

Hence, the phase current and short-circuit current can be further expressed as:

$$i = \frac{u-e}{R},\ i_{sc} = \frac{e_{sc}}{R_{sc}} = \frac{e}{R} \tag{3}$$

Generally, the ratio among the e to the terminal voltage, u is known as k, which is around 85% to 90% [30]. By substituting $k = e / u$ into (3), the expression yields:

$$i_{sc} = \frac{k}{1-k}i \tag{4}$$

It shows that short-circuit current is around 5.7 to 9 times larger than the phase current and results in larger amount of heat energy. To avoid damaging the electric motor, special cares must be provided upon the fault conditions.

A. Fault-tolerant brushless AC (FT-BLAC) operation

Traditionally, under the short-circuit fault conditions, the faulty phases can be disabled and regarded as the open-circuit fault [27]. The fault condition can then be remedied by reconstructing the remaining healthy armature phases, similar as those happen in the open-circuit fault. Even though the spatial distribution of the armature currents in the healthy phase can never be changed, the amplitude and temporal distribution of currents are controllable, hence achieving the field-reconfiguration and so-called as the FT-BLAC operation.

Similar as the convention double-salient PM (DSPM) motor, the proposed FT-FRDS motor can also work with the FT-BLAC operation with each phase having 180° conduction angle, in accordance to the conditions of the flux-linkage, Ψ_{FRDS} as shown in Fig. 2. Under the normal BLAC operation, the phase currents are four-phase sinusoidal form as given by:

$$\begin{cases} i_a = I_{\max}\cos\theta \\ i_b = I_{\max}\cos(\theta + (\pi/2)) \\ i_c = I_{\max}\cos(\theta + \pi) \\ i_d = I_{\max}\cos(\theta - (\pi/2)) \end{cases} \tag{5}$$

Because the four-phase currents are spatially displaced from each other by 90°, the rotating magnetomotive force (MMF) can be expressed as the sum of MMFs generated by four-phase currents:

$$MMF = MMF_a + MMF_b + MMF_c + MMF_d \tag{6}$$

The sum of MMFs can be further described by the spatial distribution of phase currents as:

$$MMF = Ni_a + aNi_b + a^2Ni_c + a^3Ni_d \tag{7}$$

where $a = 1 \angle -90°$ is the spatial distribution of phase currents. By substituting (5) into (7), the MMFs can be deduced as:

$$MMF = 2NI_{\max}(\cos\theta + j\sin\theta) = 2NI_{\max}e^{j\theta} \tag{8}$$

To elaborate the FT-BLAC operation, the case when the phase-a winding is under the short-circuit fault is considered. The phase-a winding can be disabled purposely such that the MMF can be reconstructed based on the three remaining healthy phase currents:

$$MMF' = MMF'_b + MMF'_c + MMF'_d \tag{9}$$

Similarly, the sum of MMFs can be further described by the spatial distribution of phase currents as:

$$MMF' = aNi'_b + a^2 Ni'_c + a^3 Ni'_d \tag{10}$$

By equating (8) and (10), two equations with three variables (i'_b, i'_c, and i'_d) are solved. To eliminate one degree of freedom, the variables are purposely related as $i'_b = -i'_d$. This ends up with the unique solution and the summation of three current phasors is zero. The remedial four-phase currents can be expressed as:

$$\begin{cases} i'_a = 0 \\ i'_b = I_{\max} \cos(\theta + (\pi/2)) \\ i'_c = 2I_{\max} \cos(\theta + \pi) \\ i'_d = I_{\max} \cos(\theta - (\pi/2)) \end{cases} \tag{11}$$

It shows that there is no spatial displacement among any phase currents in the remediation strategy, while only the amplitude of phase-c is purposely increased to 2 times larger than that of its pre-fault value.

For further exemplification, two adjacent phases, namely the phase-a, and phase-b currents, are short-circuited simultaneously. Similarly, both phases are purposely disabled and the rotating MMF is the sum of the MMFs of the remaining two phases:

$$MMF'' = MMF''_c + MMF''_d \tag{12}$$

Again, the sum of MMFs can be further described by the spatial distribution of phase currents as:

$$MMF'' = a^2 Ni''_c + a^3 Ni''_d \tag{13}$$

By equating (8) and (13), it results in the new remedial current expressions as:

$$\begin{cases} i''_a = 0 \\ i''_b = 0 \\ i''_c = 2I_{\max} \cos(\theta + \pi) \\ i''_d = 2I_{\max} \cos(\theta - (\pi/2)) \end{cases} \tag{14}$$

Again, there is no spatial displacement among any phase currents in the remediation strategy, while only the amplitude of the remaining health sets is purposely increased to 2 times larger than that of its pre-fault value.

The corresponding current phasors of the normal BLAC operation and FT-BLAC operations under different fault conditions are as shown in Fig. 3. By applying the FT-BLAC operation, the motor can be remedied to offer the pre-fault torque level. However, the armature current has to be boosted up accordingly for torque remediation. To achieve it, higher tolerant factors for the armature winding are needed and hence the material cost is increased. This problem is expected to become even more severe in the case of the multi-phase machines.

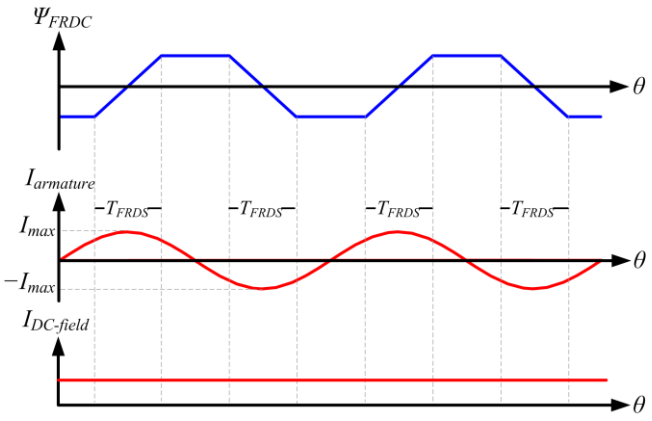

Fig. 2. Principle of proposed motor drive operations.

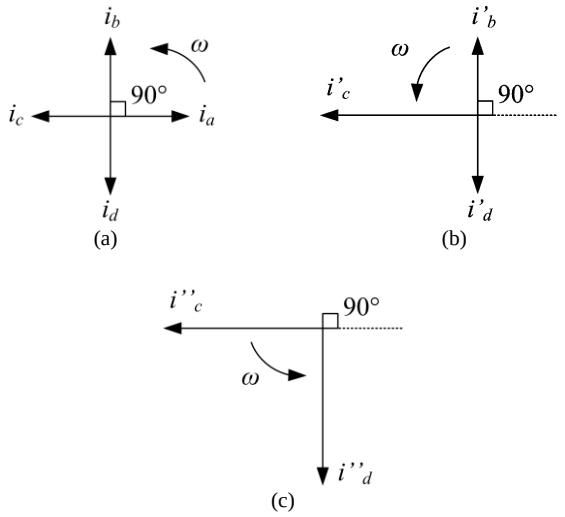

Fig. 3. Current phasor of the BLAC operations: (a) Normal BLAC operation. (b) FT-BLAC operation with 1-phase shorted. (c) FT-BLAC operation with 2-adjacent-phase shorted.

TABLE I
KEY DESIGN DATA OF THE PROPOSED MACHINE

Items	FT-FRDS
Rotor outside diameter	128.0 mm
Rotor inside diameter	100.9 mm
Stator outside diameter	100.0 mm
Stator inside diameter	22.0 mm
No. of rotor poles	10
No. of actual stator poles	8
No. of pole-pairs on stator pole	1
No. of modulated stator tooth	3
Rotor pole arc	18.0°
Stator (modulated) pole arc	12.0°
Airgap length	0.45 mm
Stack length	80.0 mm
No. of armature phases	4
No. of turns per armature coil	38

B. Fault-tolerant DC-field (FT-DC) operation

According to the derivations in previous section, namely the (11), and (14), it is confirmed that there is no spatial displacement among any healthy armature phase under the FT-BLAC operation, in every fault condition. To retrieve

the torque level, under the FT-BLAC operation, the only involvement is the amplitude of the armature currents. In order word, the FT-BLAC operation purposely regulating the airgap flux density to remedy the fault conditions.

To simplify the case and relieve the design burden of the armature phases, the fault conditions can be instead remedied by rectifying the controllable DC-field [33], and so-called as the FT-DC operation. With the application of the DC-field control, the airgap flux density can be regulated effectively, in order to achieve the similar performance as the FT-BLAC operation does. Meanwhile, the FT-DC operation can be accomplished merely by the regulation of the DC-field winding. Hence, only the DC-field winding is designed with the higher tolerant factor, while all the armature windings can be instead designed with the optimal parameters. This can improve the overall performance in the sense of the material cost aspect.

Unlike the FT-BLAC operation, which regulates the airgap flux density selectively, the FT-DC operation somehow boosts up all the remaining armature phases. This regulating technique may unfavorably boost up the non-targeted armature winding sets, hence it is expected that larger torque ripples should be resulted. Meanwhile, under the FT-DC operation, the exact value of the DC-field regulating current can hardly be found based on the mathematical model. Therefore, it is suggested to adopt the empirical approach to figure out the corresponding values.

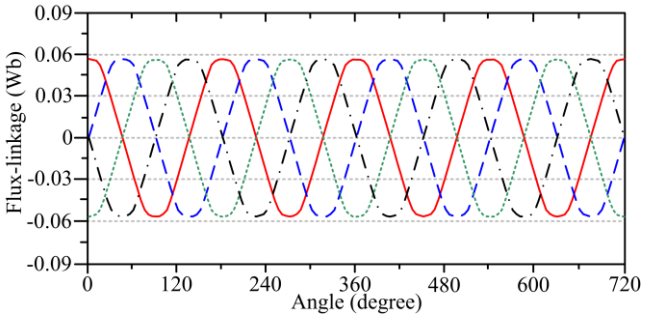

Fig. 4. Flux-linkage of the proposed motor drive.

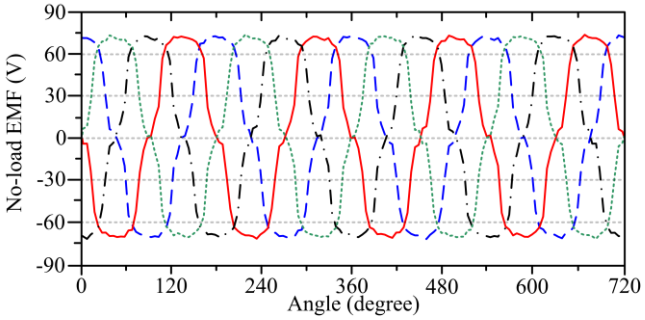

Fig. 5. No-load EMF of the proposed motor drive.

IV. Motor Drive Performance Analysis

By performing FEM, the performances of the proposed motor drive can be calculated and analyzed. The corresponding key design data of the machine are listed in Table I. Firstly, the flux-linkages of FT-FRDS are shown in Fig. 4. It can be found the flux-linkages of the armature windings are well balanced among four-phase pattern with bipolar patterns, therefore verifying the reversing flux-linkage characteristics. Secondly, the no-load EMFs of the armature windings with the DC-field excitation of 5 A at base speed 1200 rpm are shown in Fig. 5. The result illustrates that the proposed motor drive consists of the typical no-load EMF patterns, which is suitable for the conventional BLAC conduction scheme.

In the third place, the torque and current waveforms of the proposed motor drive under the normal BLAC operation, FT-BLAC operation with 1-phase shorted, and 2-adjacent-phase shorted, are as shown in Fig. 6. The results show that the average torque of the normal BLAC operation, FT-BLAC operation with 1-phase shorted, and 2-adjacent-phase shorted, are found to be around 5.98 Nm, 5.96 Nm, and 5.88 Nm, respectively. These reveal that the FT-BLAC operations can remedy the short-circuit fault and retrieve the faulty torque level as that of the normal operation does.

Fourthly, the average torques under the FT-DC operation in variants to the DC-field excitations under different fault conditions, namely 1-phase shorted, and 2-adjacent-phase shorted, are as shown in Fig. 7. As confirmed, the fault conditions can be remedied by the regulation of the DC-field, and the torque levels can be retrieved accordingly. In particular, the regulated DC-field excitations under 1-phase shorted, and 2-adjacent-phase shorted, are found to be 6.7 A, and 9.8 A, respectively.

Fifthly, the waveforms of the steady torque of FT-DC operation under different fault conditions, namely 1-phase shorted, and 2-adjacent-phase shorted, are as shown in Fig. 8, respectively. The results show that the average torques of the FT-DC operation with 1-phase shorted, and 2-adjacent-phase shorted, are found to be around 5.97 Nm, and 5.93 Nm, respectively. Hence, further confirming the FT-DC operation can remedy the fault conditions and maintain the torque levels within the normal range.

Finally, to offer the more comprehensive comparisons, the torque ripple values are also studied and the so-called torque ripple factor, K_T is defined as following:

$$K_T = \frac{T_{\max} - T_{\min}}{T_{avg}} \times 100\% \qquad (15)$$

where T_{max}, T_{min}, and T_{avg} are the maximum, minimum and average torque produced, respectively. According to the results, the torque ripples under normal BLAC, FT-BLAC operations with 1-phase shorted, and 2-phase shorted, are around 33.4 %, 37.2 %, and 38.3 %, respectively. Meanwhile, the torque ripples under the FT-DC operations with 1-phase shorted, and 2-phase shorted, are around 64.5 %, and 47.5 %, respectively. Undoubtedly, without any fault condition, in term of the torque ripple performances, the normal BLAC operation outperforms the other two remedial operations. Meanwhile, due to the selective regulation of the particular armature sets, the torque ripple values under the FT-BLAC operation is smaller than that of the FT-DC operations do. However, the multi-phase machines under the FT-DC operation can enjoy the better

material utilization as compared with those machines adopt with the FT-BLAC operation do.

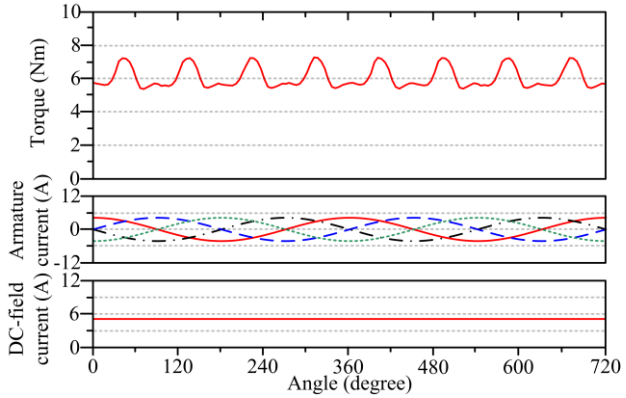

(a)

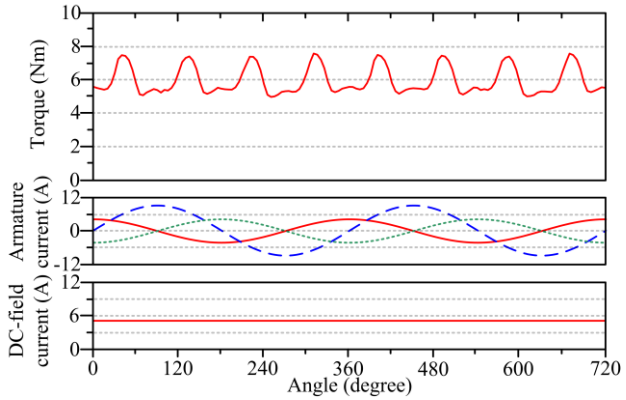

(b)

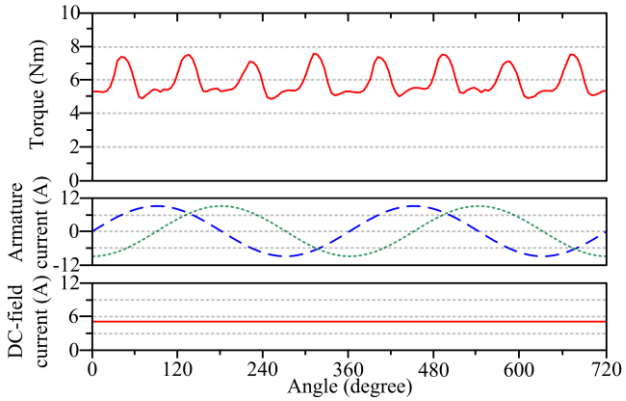

(c)

Fig. 6. Torque waveforms at BLAC operation: (a) Normal. (b) 1-phase under short-circuit fault. (c) 2-adjacent-phase under short-circuit fault.

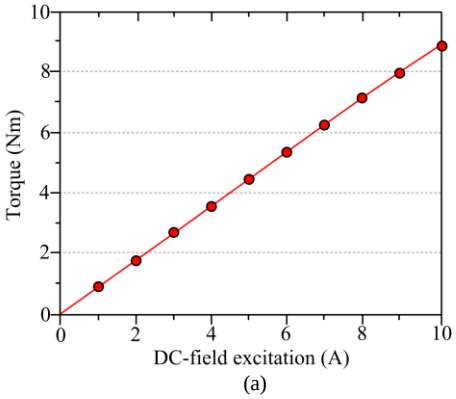

(a)

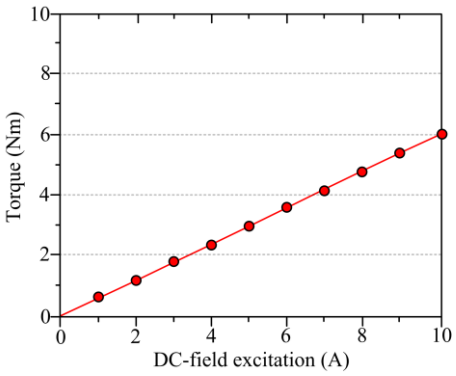

(b)

Fig. 7. Average torque characteristics based on the variations of the DC-field excitation: (a) 1-phase under short-circuit fault. (b) 2-adjacent-phase under short-circuit fault.

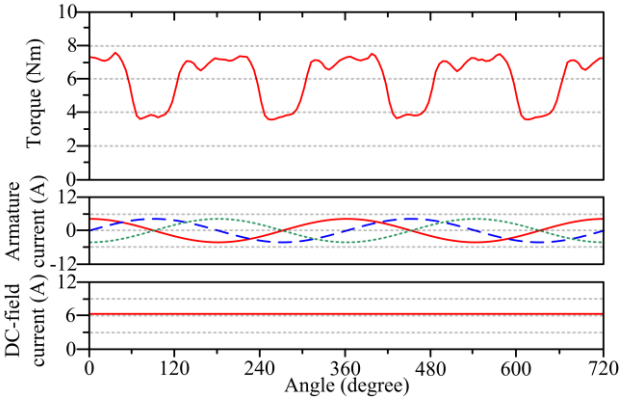

(a)

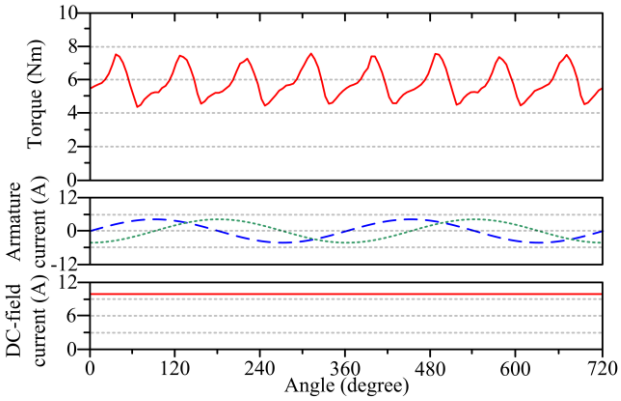

(b)

Fig. 8. Torque waveforms at FT-DC operation: (a) 1-phase under short-circuit fault. (b) 2-adjacent-phase under short-circuit fault.

TABLE II
TORQUE PERFORMANCE COMPARISONS

Operation mode	Average torque	Torque ripple	Peak phase current	Field current
Normal BLAC	5.98Nm	33.4 %	5 A	5 A
FT-BLAC (1-phase shorted)	5.96 Nm	37.2 %	10 A	5 A
FT-BLAC (2-phase shorted)	5.88 Nm	38.3 %	10 A	5 A
FT-DC (1-phase shorted)	5.97 Nm	64.5 %	5 A	6.7 A
FT-DC (2-phase shorted)	5.93 Nm	47.5 %	5 A	9.8 A

V. Conclusion

In this paper, a new magnetless FT-FRDS motor drive with high fault tolerance capability has been proposed and verified by FEM. Different operations, namely the normal BLAC, FT-BLAC and FT-DC operations are quantitatively compared and the results are summarized in Table II. By purposely reconstructing the armature currents or regulating the DC-field currents, the short-circuit faults are remedied and the torque levels can be maintained as the normal condition does. In terms of the torque ripple values, the FT-BLAC operation outperforms the FT-DC one. Meanwhile, in the machine design aspects, the FT-DC operation provides the potentiality to have the better material utilization, and hence better overall performances.

VI. References

[1] C. C. Chan and K.T. Chau, *Modern Electric Vehicle Technology*. Oxford University Press, Nov. 2001.

[2] C. C. Chan, "The state of the art of electric and hybrid vehicles," *Proc. IEEE*, vol. 90, no. 2, pp. 247–275, Feb. 2002.

[3] Z. Q. Zhu, and D. Howe, "Electrical machines and drives for electric, hybrid, and fuel cell vehicles" *IEEE Proc.*, vol. 95, no. 4, pp. 746–765, Apr. 2007.

[4] K. T. Chau, W. Li, and C. H. T. Lee, "Challenges and opportunities of electric machines for renewable energy," *Prog. Electromagn. Res. B*, vol. 42, pp. 45–74, 2012.

[5] K. T. Chau, C. C. Chan and C. Liu, "Overview of permanent-magnet brushless drives for electric and hybrid electric vehicles," *IEEE Trans. Ind. Electron.*, vol. 55, no. 6, pp. 2246–2257, June 2008.

[6] R. Cao, C. Mi, and M. Cheng, "Quantitative comparison of flux-switching permanent-magnet motors with Interior permanent magnet motor for EV, HEV, and PHEV applications," *IEEE Trans. Magn.*, vol. 48, no. 8, pp. 2374–2384, Dec. 2008.

[7] C. Liu, K. T. Chau, and J. Z. Jiang, "A permanent-magnet hybrid brushless integrated-starter-generator for hybrid electric vehicles," *IEEE Trans. Ind. Electron.*, vol. 57, no. 12, pp. 4055–4064, Dec. 2010.

[8] W. Li, K.T. Chau, Y. Gong, J.Z. Jiang and F. Li, "A new flux-mnemonic dual-magnet brushless machine," *IEEE Trans. Magn.*, vol. 47, no. 10, pp. 4223–4226, Oct. 2011.

[9] Y. Du, M. Cheng, K.T. Chau, X. Liu, F. Xiao, and W. Zhao, "Linear primary permanent magnet vernier machine for wave energy conversion," *IET Electr. Power Appli*., vol. 9, no. 3, pp. 203–212, Mar. 2015.

[10] R. P. Deodhar, S. Andersson, I. Boldea, and T. J. E. Miller "The flux-reversal machine: a new brushless doubly-salient permanent-magnet machine" *IEEE Trans. Ind. Electron*., vol. 33, no. 4, pp. 925–934, Jul. 1997.

[11] C. Liu, K. T. Chau, J. Z. Jiang, and S. Niu "Comparison of stator-permanent-magnet brushless machines," *IEEE Trans. Magn.*, vol. 44, no. 11, pp. 4405–4408, Nov. 2008.

[12] Y. Du, K.T. Chau, M. Cheng, Y. Fan, Y. Wang, W. Hua and Z. Wang, "Design and analysis of linear stator permanent magnet vernier machines," *IEEE Trans. Magn.*, vol. 47, no. 10, pp. 4219–4222, Oct. 2011.

[13] M. Cheng, W. Hua, J. Zhang, and W. Zhao, "Overview of stator-permanent magnet brushless machines," *IEEE Trans. Ind. Electron.*, vol. 58, no. 11, pp. 5087–5101, Nov. 2011.

[14] X. Li, K.T. Chau, and M. Cheng, "Comparative analysis and experimental verification of an effective permanent-magnet vernier machine," *IEEE Trans. Magn.*, vol. 51, no. 7, paper no. 8203009, pp. 1–9, Jul. 2015.

[15] C. H. T. Lee, K. T. Chau, C. Liu, D. Wu, and S. Gao, "Quantitative comparison and analysis of magnetless machines with reluctance topologies," *IEEE Tran. Magn.*, vol. 49, no. 7, pp. 3969–3972, Jul. 2013,

[16] M. Chen, K. T. Chau, W. Li, and C. Liu "Cost-effectiveness comparison of coaxial magnetic gears with different magnet materials," *IEEE Trans. Magn.*, vol. 50, no. 2, p. 7020304, Feb. 2014.

[17] W Li, K.T. Chau, C. Liu and C. Qiu, "Design and analysis of a flux-controllable linear variable reluctance machine," *IEEE Trans. Appl. Supercond*., vol. 24, no. 3, paper no. 5200604, pp. 1–4, Jun. 2014.

[18] C. H. T. Lee, K. T. Chau, C. Liu, T. W. Ching and F. Li, "A High-Torque Magnetless Axial-Flux Doubly-Salient Machine for In-Wheel Direct Drive Applications," *IEEE Tran. Magn.*, vol. 50, no. 11, p. 8202405, Nov. 2014.

[19] Y. Wang, J. Sun, Z. Zou, Z. Wang, and K. T. Chau, "Design and analysis of a HTS flux-switching machine for wind energy conversion," *IEEE Trans. Appl. Supercond.*, vol. 23, no. 3, p. 5000904, Jun. 2013.

[20] C. H. T. Lee, C. Liu, and K. T. Chau, "A magnetless axial-flux machine for range-extended electric vehicle," *Energies*, vol. 7, no. 3, pp. 1483–1499, Mar. 2014.

[21] X. Liu, and Z. Q. Zhu, "Stator/rotor pole combinations and winding configurations of variable flux reluctance machines," *IEEE Trans. Ind. Appl*., vol. 50, no. 6, p. 3675–3684, Apr. 2014.

[22] C. H. T. Lee, K. T. Chau, C. Liu, T. W. Ching, and F. Li, "Mechanical offset for torque ripple reduction for magnetless double-stator doubly-salient machine," *IEEE Tran. Magn.*, vol. 50, no. 11, pp. 8103304, Nov. 2014.

[23] C. Liu, K. T. Chau, C. H. T. Lee, F. Lin, F. Li, and T. W. Ching, "Magnetic vibration analysis of a new DC-excited multitoothed switched reluctance machine," *IEEE Tran. Magn.*, vol. 50, no. 11, p. 8105204, Nov. 2014.

[24] C. H. T. Lee, K. T. Chau, and C. Liu, "Design and analysis of a dual-mode flux-switching doubly salient DC-field magnetless machine for wind power harvesting," *IET Renew. Power Gener.*, accepted.

[25] C. H. T. Lee, K. T. Chau, C. Liu, T. W. Ching, and M. Chen, "A new magnetless flux-reversal HTS machine for direct-drive application," *IEEE Trans. Appl. Supercond.*, vol. 25, no. 3, p. 5203105, Jan. 2015.

[26] C. H. T. Lee, K. T. Chau, and C. Liu, "Design and Analysis of a cost-effective magnetless multi-phase flux-reversal DC-field machine for wind power generation," *IEEE Tran. Energy Convers*., accepted.

[27] N. Bianchi, S. Bolognani, and M. Dai Pre´, "Strategies for the fault-tolerant current control of a five-phase permanent magnet motor," *IEEE Trans. Ind. Appl*., vol. 43, no. 4, pp. 960–970, Jul. 2007.

[28] W. Zhao, K. T. Chau, M. Cheng, J. Ji, and X. Zhu, "Remedial brushless AC operation of fault-tolerant doubly-salient permanent-magnet motor drives," *IEEE Trans. Ind. Electron.*, vol. 57, no. 6, pp. 2134–2141, Jun. 2010.

[29] F. Lin, K. T. Chau, C. H. T. Lee, and C. Liu, "Fault signature of a flux-switching DC-field generator," *IEEE Tran. Magn.*, accepted.

[30] C. Yu, and K. T. Chau, "New fault-tolerant flux-mnemonic doubly-salient permanent-magnet motor drive," *IET Electr. Power Appl.*, vol. 5, pp. 393–403, May 2011.

[31] W. Zhao, M. Cheng, K.T. Chau, R. Cao and J. Ji, "Remedial injected harmonic current operation of redundant flux-switching permanent magnet motor drives," *IEEE Trans. Ind. Electron.*, vol. 60, no. 1, pp. 151–159, Jan. 2013.

[32] F. Lin, K.T. Chau, C.C. Chan, and C. Liu, "Fault diagnosis of power components in electric vehicles," Journal of Asian Electric Vehicles, vol. 11, no. 2, pp. 1659–1666, Dec. 2013.

[33] C. Liu, K. T. Chau, and W. Li, "Comparison of fault-tolerant operations for permanent-magnet hybrid brushless motor drive," *IEEE Tran. Magn.*, vol. 46, no. 6, pp. 1378–1381, Jun. 2010.